



**HAL**  
open science

# Reassessment of paleointensity estimated of a single lava flow from Xitle volcano, Mexico, by means of multispecimen domain-state corrected

L.M. Alva-Valdivia, M.A. Bravo-Ayala, P. Camps, A.N. Mahgoub, Thierry Poidras

## ► To cite this version:

L.M. Alva-Valdivia, M.A. Bravo-Ayala, P. Camps, A.N. Mahgoub, Thierry Poidras. Reassessment of paleointensity estimated of a single lava flow from Xitle volcano, Mexico, by means of multispecimen domain-state corrected. *Journal of South American Earth Sciences*, 2020, 100, pp.102549. 10.1016/j.jsames.2020.102549 . hal-02871023

**HAL Id: hal-02871023**

<https://hal.umontpellier.fr/hal-02871023v1>

Submitted on 31 Jul 2020

**HAL** is a multi-disciplinary open access archive for the deposit and dissemination of scientific research documents, whether they are published or not. The documents may come from teaching and research institutions in France or abroad, or from public or private research centers.

L'archive ouverte pluridisciplinaire **HAL**, est destinée au dépôt et à la diffusion de documents scientifiques de niveau recherche, publiés ou non, émanant des établissements d'enseignement et de recherche français ou étrangers, des laboratoires publics ou privés.

1 Multispecimen domain-state corrected paleointensity determination of a  
2 detailed single lava flow, Xitle volcano (Mexico)

3  
4  
5 L. M. Alva-Valdivia<sup>1\*</sup>, M. A. Bravo-Ayala<sup>1</sup>, P. Camps<sup>2</sup>, A. N. Mahgoub<sup>1,3</sup>, and Thierry  
6 Poidras<sup>2</sup>

7  
8  
9 <sup>1</sup> Laboratorio de Paleomagnetismo, Instituto de Geofísica, Universidad Nacional Autónoma  
10 de México, C.P. 04510, Coyoacán, México

11 <sup>2</sup> Géosciences Montpellier, CNRS and University Montpellier, Montpellier, France

12 <sup>3</sup> Geology Department, Assiut University, Assiut 71516, Egypt

13  
14 \*Corresponding author: lalva@igeofisica.unam.mx

15  
16  
17 **Abstract**

18 Determining paleomagnetic field intensity (paleointensity: PI) for lavas with high reliability  
19 and low measurement uncertainty is still difficult to achieve. In addition to the factors on  
20 which the PI used methods depend, this could be attributed to some non-ideal physical and  
21 magnetic characteristics of lava sample, including grain size, cooling rate effect, and thermal  
22 stability. Xitle volcano (SW Mexico City) is a good example to illustrate and discuss this  
23 problem because dozens of previous PI studies were carried out on its evolved flow units,  
24 which have commonly resulted in different mean values with large dispersions. Indeed, 211  
25 published PI data obtained by use of Thellier and microwave experiments gave a mean of  
26  $64.1 \mu T$  with a standard deviation of  $11.0 \mu T$ . After a careful evaluation, we found that only  
27 134 of these data can be considered reliable, as they meet a set of selection criteria designed

28 in this study. These evaluated data gave an average mean of  $62.0 \pm 9.3 \mu T$ . In order to  
29 strengthen the PI estimates of Xitle, we conducted a multispecimen domain-state corrected  
30 (MSP-DSC) method along one vertical ( $\sim 4.5\text{m}$ ) and three horizontal ( $\sim 1.25\text{m}$ , each)  
31 profiles. Top horizontal and vertical profiles have fulfilled a stringent criteria set while central  
32 and bottom profiles exceeded the alteration check criteria limit and thus are considered  
33 unreliable. Accordingly, Xitle PI mean derived from MSP-DSC experiment is calculated at  
34  $60.5 \pm 4 \mu T$ , thus in a good agreement with the mean value estimated from previous filtered  
35 data. The result and success rate obtained may be ascribed to cooling rate variations  
36 commonly found at the lava profile, and indicate that MSP-DSC outcome is governed by the  
37 magnetic properties such as the domain-size behavior and the thermal stability of the  
38 magnetic carriers present in the treated specimens, as in the conventional Thellier &  
39 microwave-style experiments. From these two averages, a combined mean and standard  
40 deviation of  $61.9 \pm 9 \mu T$  is calculated, which technically is considered the most probable  
41 intensity estimate at the Xitle eruption time, *ca.* 370 AD.

42 Keywords: paleointensity; lavas; rock magnetic properties; multispecimen method; Xitle;  
43 Mexico

44  
45  
46

## 47 **1. Introduction**

48 Over the long history of our planet, the magnetic field generated in the liquid outer core  
49 changed on different time scales from years to billions of years. Understanding the spatio-  
50 temporal evolution of this field requires careful determination of its strength. Because of its  
51 large contributions in deciphering the geodynamo behavior (Biggin et al., 2012) and  
52 improving the global geomagnetic field models (e.g., SHA.DIF.14k, Pavón-Carrasco et al.,  
53 2014), several methods were proposed to obtain a reliable estimate of the PI: the classical

54 Thellier-Thellier experiment (Thellier & Thellier 1959) and other protocols (e.g., Coe et al.,  
55 1967; Aitken et al., 1988; Tauxe and Staudigel, 2004); the Shaw method (Shaw, 1974) and  
56 its variants (e.g. Tsuanakawa and Shaw, 1994); pseudo-Thellier (Tauxe et al., 1995); the  
57 microwave technique (Hill & Shaw 1999); and the recent approach of multispecimen  
58 (Biggins and Poidras, 2006; Dekkers and Böhnel, 2006; Fabian and Leonhardt, 2010).  
59 Despite the improvements achieved in the laboratory protocols, these methods give reliable  
60 intensity with a low success rate (generally less than 30%) from basalts, the material of  
61 interest in this study. This was showed by comparing PI data retrieved from historically  
62 erupted lava flows, such as those in Hawaii (e.g. Yamamoto et al., 2003; Böhnel et al., 2011;  
63 Grappone et al., 2019) and Etna (e.g. Hill and Shaw, 1999; De Groot et al., 2013), with the  
64 actual geomagnetic field intensity that is well known from geomagnetic observatories. Th  
65 elow success rate in the PI methods to recover the expected field intensity with high accuracy  
66 could be attributed to several reasons, including the presence of non-ideal physical and  
67 magnetic properties, magneto-mineralogical alteration, the cooling rate difference and  
68 presence of local magnetic field effects (Stacey & Banerjee 1974). From the PI point of view,  
69 lava samples must contain ferromagnetic particles of single domain (SD;  $< \sim 80$  nm) to  
70 pseudo-SD (PSD;  $< \sim 0.1$   $\mu\text{m}$ ) size . This condition however, is not easily reached because in  
71 naturally cooled lavas there are always contributions from grains larger than  $\sim 1.0$   $\mu\text{m}$ , of  
72 multidomain (MD) size. In this context, Cromwell et al. (2015) have showed the capability  
73 of subaerial basaltic volcanic glass to give accurate field intensity as they have cooled quickly  
74 and behaves as SD particles. Unfortunately, these glassy samples are not usually available,  
75 but indeed the most commonly encountered material is a lava flow which depends on its

76 position and cooling rate can take from days to several months to cool, and thus a wide range  
77 of domain size is expected.

78 All these factors may be responsible for over- or under-estimating the PI values. Xitle lava  
79 flows (Fig. 1) allowed to illustrate and discuss this problem because dozens of previous PI  
80 estimates conducted on them have commonly yielded different mean values with large  
81 dispersions . These data were mainly obtained by means of Thellier method and some others  
82 were provided by means of microwave and Shaw techniques. It should be mentioned here  
83 that previous data are of uneven quality and thus in the next section we will discuss their  
84 reliability based on today's set criteria parameters (Paterson et al., 2014; Thellier et al., 2014).  
85 The present work was designed to reinforce Xitle PI estimates and to reduce its errors through  
86 applying MSP-DSC method along one vertical (*ca.* 4.5m) and three horizontal profiles.  
87 Providing a new reliable PI value for a dated flow unit is important to (among others) enhance  
88 the global harmonic spherical models of the secular variation of the geomagnetic field over  
89 the last millennia (e.g. Nilsson et al., 2014 and Pavón-Carrasco et al., 2014) and improve our  
90 knowledge of the local field intensity behavior in central Mexico at *ca.* 370 AD.

## 91 **2. Geological setting and sampling**

92 The study profile (19.328° N; 99.189° W) is part of the flow VI of Xitle (Fig. 1) located  
93 inside the campus of UNAM (Universidad Nacional Autónoma de Mexico). Xitle lies in the  
94 central sector of the Trans-Mexican Volcanic Belt (TMVB, Fig. 1) which is an E–W trending  
95 zone of *ca.*1000 km length extending from the Pacific Ocean to the Gulf of Mexico. The  
96 TMVB is divided in western, central, and eastern sectors. The Sierra de Chichinautzin  
97 Volcanic Field (SCVF) is located in the central sector (inset Fig. 1).

98 The SCVF contains high concentration of monogenetic volcanoes with about 220 Quaternary

99 volcanic products including cinder cones and lava flows (Siebe, 2000; Rodríguez-Trejo et  
100 al., 2019) of wide compositional range. Xitle is considered as the youngest monogenetic  
101 volcano of the SCVF with a radiocarbon age of 1530-1630 uncalibrated yr BP (cal.  $370\pm 60$   
102 AD; Siebe et al., 2004; Arce et al., 2013). Xitle eruption is an example of the impact of  
103 volcanic disaster on the human population, as supposedly it had damaged the pre-Hispanic  
104 settlements around Cuicuilco pyramid (Fig. 1) which prompted them to emigrate (Siebe,  
105 2000), as like in the historical eruptions of the Jorullo (1759–1774 AD; Guilbaud et al., 2011;  
106 Rasoazanamparany et al., 2016; Alva-Valdivia et al., 2019) and Paricutin (1943–1952 AD;  
107 Luhr and Simkin, 1993; Pioliet al., 2008) monogenetic volcanoes.

108 The sampled site was selected so that the bottom and top of the lava section (Fig. 3) are  
109 visible. Sampling was done using a portable gasoline powered drill, and 72 core samples,  
110 each with 5-10 cm long and 2.5 cm diameter, were collected. In this study, four profiles (Fig.  
111 3) were taken and distributed as follow: one vertical profile (V) of *ca.* 4.5 m thickness and  
112 composed of 43 cores; and three horizontal profiles (H) of *ca.* 1.25 m length for each: top  
113 horizontal (HT) of 11 cores; middle horizontal (HM) of 10 cores; and the bottom horizontal  
114 (HB) of 11 cores.

### 115 **3. Previous PI studies**

116 Nine PI studies were conducted on Xitle lava flows by means of the double heating Thellier  
117 (Nagata et al., 1965; Urrutia-Fucugauchi, 1996; Gonzales et al., 1997; Alva Valdivia, 2005;  
118 Böhnell et al., 1997; Morales et al., 2001, 2006; Mahgoub et al., 2019); microwave (Böhnell  
119 et al., 2003); and Shaw (Urrutia-Fucugauchi, 1996; Gonzales et al., 1997) methods. Sampling  
120 in five of these studies were collected randomly and its coordinates are of low precision  
121 which makes us unable to define target flow unit in some of them. On the other hand, three

122 studies (Böhnel et al. , 1997; 2003; Alva-Valdivia et al., 2005) were designed so as to sample  
123 vertical profiles over a specific cooling unit.

124 Two studies (Böhnel et al., 2003; Mahgoub et al., 2019) were carried out on pottery fragments  
125 that were reheated by Xitle eruption and thus acquired their magnetization at the same time.  
126 Böhnel et al. (2003) have performed microwave experiments on lavas and pottery fragments,  
127 with the field applied perpendicular and parallel to the their NRM. We note also that PI data  
128 points presented in Böhnel et al. (1997) have been re-analyzed by Böhnel et al. (2003)  
129 applying a stringent set of selection criteria. At this point, it must be stated that Böhnel et al.  
130 (1997) carried out their study rather to find out how PI varies over the Xitle flow (see section  
131 5.2) and if there is a relation between rock magnetic properties and success rate, therefore  
132 they have not used a very strict selection criteria. Morales et al. (2006) tried to figure out the  
133 cause of PI dispersion through conducting cooling rate correction. Based on their results, a  
134 significant decrease in PI-dispersion was obtained (from 7.5 to 3.5  $\mu\text{T}$ ), thus they have  
135 claimed that cooling-rate effect may have a prominent role in the observed dispersion. There  
136 are two points to be mentioned in this context: the first is that Morales et al. (2006) have  
137 obtained positive and negative corrections from nearby samples (of 10-20 cm distance) that  
138 should have a very similar cooling rate. Secondly, if the change in the cooling rate is the  
139 reason for the PI-dispersion, then, reasonably, Thellier results will give less scatter than  
140 microwave approach, as the duration of each microwave step is *ca.* 10 seconds (Hill and  
141 Shaw, 1999). Böhnel et al. (2003), though using microwave technique on a nearby profile,  
142 provided PI mean results with similar dispersion as commonly obtained in Thellier. These  
143 two points most likely rule out the effect of cooling rate as a major cause of intensity variation  
144 acquired from Xitle volcano.

145 In order to demonstrate the PI mean and scatter in each study and to illustrate the consistency  
146 between different studies, we plot the PI data at specimen level on Figure 2. They are 214  
147 data points [211 derived from Thellier and microwave and 3 from Shaw method] considered  
148 acceptable by the author(s) of each work. As Figure 2 illustrates, the data from each study is  
149 highly scattered and the whole data are inconsistent as well. We note that the PI-dispersion  
150 of these studies cannot be compared as the number of data is not equal: half of data were  
151 obtained by Böhnelt et al. (1997) and Alva-Valdivia et al. (2005) while Urrutia-Fucugauchi  
152 (1996) and Gonzalez et al. (1997) provided only 3 PI data points using Shaw technique. Using  
153 all data, we calculate Xitle PI mean at 64.1  $\mu\text{T}$  (Fig. 2) and the 95% standard deviation ( $\sigma$ ) is  
154 11  $\mu\text{T}$ , *ca.* 18% of the mean. Since the number of data is generously available and meet the  
155 suggestion of Biggin et al. (2003) that PI mean value of any lava flow should be based on as  
156 many samples as possible (at least five). Apparently this dispersion could be related to,  
157 among others, some problems in the experimental PI methods (especially those applied long  
158 time ago). We evaluate previous 211 Thellier and microwave - derived PI data in terms of  
159 recently proposed reliability standards (e.g. Tauxe and Staudigel 2004; Chauvin et al., 2005;  
160 Paterson et al., 2014). There are some other problems that could be seriously responsible for  
161 such dispersion, including alteration of the ferromagnetic particles, cooling rate effect, and  
162 presence of local magnetic field effects. These effects will not be addressed here.

163 Besides the low number of provided data, the two studies that used Shaw experiment  
164 (Urrutia-Fucugauchi, 1996; Gonzalez et al., 1997) cannot be considered reliable as they did  
165 not perform alteration tests (e.g. Tsunakawa and Shaw, 1994). In Thellier experiments,  
166 samples are heated up gradually from low (e.g. 100 °C) to high temperature (commonly  
167 below curie point) and the natural remanent magnetization (NRM) is consecutively replaced



168 by laboratory induced thermal remanent magnetization (TRM), in a known laboratory field.  
169 This must be done with some alteration checks (Coe et al., 1978) in order to ensure that no  
170 alteration occurred during repeated heating. Laboratory procedure of microwave method is  
171 the same as Thellier but instead of heating in a conventional oven, samples are demagnetized  
172 by exposure to high-frequency microwave (Walton et al., 1993). It has been proved by Hill  
173 et al. (2002) that microwave demagnetization is equivalent to thermal counterparts implying  
174 that sample's NRM is replaced by a laboratory induced TRM, for further details we refer to  
175 the work of Hill and Shaw (2000) and Böhnel et al. (2003). Due to similarity in experimental  
176 approaches, we have set for PI data derived from Thellier and microwave the same criteria  
177 set, which are:

- 178 1) Treated sample must have been checked for thermal alteration during heating by means of  
179 the pTRM check criterions ( $\delta CK$  and/or  $\delta pal$ );
- 180 2) The stability of the sample's NRM directions during the experiments must have been  
181 evaluated by one or all next parameters: MADanc,  $\alpha$ , or DANG;
- 182 3) Following Biggin et al. (2003) suggestion, at least 5 specimens must have been used to  
183 compute lava flow mean intensity with  $\sigma \leq 10 \mu T$  or  $\leq 20\%$  of the mean.

184 Applying these criteria set, we found that data presented in the work of Nagata et al. (1965),  
185 Urrutia-Fucugauchi (1996), Gonzalez et al. (1997), Böhnel et al. (1997), Morales et al. (2001)  
186 do not satisfy the mentioned criteria (Fig. 2). On the other hand, studies of Böhnel et al.  
187 (2003), Alva Valdivia (2005), Morales et al. (2006), and Mahgoub et al. (2019) are reliable.  
188 We calculate the Xitle mean PI from the 134 data considered as reliable data at  $62.0 \mu T$  with  
189  $\sigma$  of  $9.3 \mu T$  (see Fig. 2). This mean value is slightly below the mean calculated from all data

190 and the error is also reduced, however statistically they are indistinguishable at the 95%  
191 confidence limit.

#### 192 **4. Methods**

193 Rock magnetic experiments represented by the susceptibility versus temperature ( $k$ -T)  
194 analyses and hysteresis measurements were done on 2-3 samples from each sampled profile  
195 in order to check the magnetic variability in both horizontal and vertical directions.  
196 Alternating field (AFD) and thermal demagnetization (THD) were measured in all the  
197 samples of each profile.  $k$ -T curves were carried out up to  $\sim 700^\circ\text{C}$  with a Bartington-MS2  
198 susceptibility-meter coupled with the furnace XXXX (????), and the mean Curie temperature  
199 ( $T_c$ ) were defined as the inflection point after peaks in  $k$ . We evaluate the thermal alteration  
200 that could occur during the laboratory heating by calculating a reversibility  
201 parameter:  $RP\% = \frac{k_h - k_c}{k_h} * 100$ ; where  $k_h$  and  $k_c$  represent values of  $k$  at heating and cooling  
202 curves at  $100^\circ\text{C}$ , respectively (reference ???). Zero RP% indicates that the heated specimen  
203 does not experience alteration. Hysteresis analyses were executed with the AGFM  
204 (Alternating Gradient Force Magnetometer) for which samples weighting 5 to 40 mg were  
205 used. The hysteresis parameters (saturation magnetization ( $M_s$ ); saturation remanent  
206 magnetization ( $M_{rs}$ ); coercive force ( $H_c$ ); and coercivity of remanence ( $H_{cr}$ )) lead to have  
207 an idea of the magnetic domain state of the magnetic carriers, Day diagram (Day et al., 1977).  
208 AFD measurements were progressively applied from 5 to 100 mT with an AGICO LDA-3  
209 equipment. Also, THD was carried out with ASC TD-48 thermal demagnetizer model in  
210 every  $50^\circ\text{C}$  from 100 to  $500^\circ\text{C}$  and then from 530 to  $600^\circ\text{C}$  in  $30^\circ\text{C}$  step. From the  
211 demagnetization measurements, we have calculated the median destructive field (MDF) and  
212 median destructive temperature (MDT), which defined how the alternating field and

213 temperature values of the NRM loses half of its value.

214 PI experiments were estimated with the multispecimen method (Dekkers and Böhnel, 2006)

215 through which specimens are heated only once in different DC fields directed, independently,

216 parallel to the their NRM. The original protocol includes two steps: m0 and m1. Thereafter,

217 two additional steps (m2 and m3) were proposed by Fabian and Leonhardt (2010) in order to

218 correct for the domain state effect, and one more step (m4), where we repeat m1, is proposed

219 to check for any mineralogical alteration occurred during the experiment. In this study, 37

220 specimens were taken from all profiles to conduct the original (MSP-DB; referred to Dekkers

221 and Böhnel) and corrected (MSP-DSC; referred to domain state correction) protocols.

222 Heatings were carried out by use of a new infra-red-heating ultra-fast furnace developed and

223 available in the Geosciences Montpellier laboratory, called 'FURemAG'. The heating-

224 cooling time in the FURemAG furnace lasts 45 minutes. Based on the *k*-T curves and THD

225 results, the set-temperature will be selected so as to ensure unblocking sufficient portion of

226 NRM. Thus, we can get steeped linear fit with small confidence limit (Monster et al., 2015a),

227 and also magneto-mineralogical alteration can be avoided. To eliminate unwanted viscous

228 component in the NRM, the specimens were heated to 100°C and cooled to room temperature

229 in zero field, before the NRM measurement (m0 step). To be consistent with this pre-

230 treatment, the low temperature pTRM[100°C, Troom] was removed in the same way after

231 each pTRM acquisition (m1, m2, m3, and m4 steps) involved in the MSP-DSC protocol. The

232 magnetic remanence was measured with a cryogenic magnetometer (2G).

## 233 **5. Results**

### 234 ***5.1 Magnetic properties***

235 The *k*-T curves (Figs.4a) indicate the presence of several magnetic minerals in distinct

236 proportion. The Tc range from 540 to > 600 °C and RP% from 4 to 80%, suggesting the

237 presence of magnetite (Mag), Ti-poor titanomagnetite (Ti-poor TMag), and hematite with  
238 varied reversibility degrees. In all studied samples,  $k$  value decrease after heating, indicating  
239 that enclosed magnetic minerals have been oxidized. We found that both  $T_c$  and RP% do not  
240 have any systematic behavior vertically or horizontally, but we can mention that HT and HM  
241 profiles have moderate to good reversibility, respectively. Specimens of HB gave dissimilar  
242 results and thus no clear conclusion can be outlined.

243 Hysteresis analyses show that all investigated samples are located in the range of PSD field  
244 (Fig. 4b), which may suggest presence of a mixture of SD and MD particles in different  
245 percentages. HT samples are located close together in the Day plot while those of HM and  
246 HB did not show similar consistency. We deduced from these observations that HT profile  
247 has a small homogenous PSD particles while, on the other hand, the middle and bottom  
248 profiles have somewhat larger ferromagnetic particles of widespread type and/or size.  
249 Apparently, few samples are provided this explanation and thus more samples would lead to  
250 track better the domain state along vertical and horizontal profiles. However, the recent  
251 findings of Roberts et al. (2018) should be mentioned where they find out that domain state  
252 of a sample cannot be grasped simply from the Day plot as the hysteresis parameters are  
253 based on several variables (Roberts et al., 2018).

254 Intensity-decay curves along the three horizontal profiles results from AFD measurements  
255 (Fig. 4c) do not show any systematic behavior (as in previous experiments), and the MDF  
256 ranges from 5 to 55 mT thus indicating the presence of varying magnetic grain composition  
257 along the three sampled profiles. The THD data (Fig. 4d) showed the appearance of common  
258  $T_c$  point of magnetite (*ca.* 560°C) with small contribution from hematite, thus in agreement  
259 with  $k$ -T curves. The MDTs are from 300 to 500 °C with a tendency of HB's samples (58,

260 59 and 64) to have lower MDT in comparison to HT and HM. This tendency could be  
261 attributed to the presence of different Ti contents (as they have low unblocking temperature  
262 spectra) or to large magnetic minerals size in the HB samples.

263 To sum up, magnetic experiments showed that rock from the sampled profiles, although of  
264 limited vertical and horizontal spread, have wide range of type composition and size of the  
265 enclosed magnetic minerals.

## 266 *5.2 MSP-DSC results*

267 The multispecimen data corrected for domain state (MSP-DSC) were analyzed with MSP-  
268 Tool (Monster et al., 2015) software. The set-temperature throughout the experiments is  
269 400°C and applied DC fields range from 10 to 80  $\mu\text{T}$ . The domain state proxy ( $\alpha$ -parameter)  
270 was set to 0.5, as proposed by Fabian and Leonhardt (2010). Credibility of the MSP results  
271 were checked by three parameters: thermal-induced alteration  $|\varepsilon_{\text{alt}}|$  parameter (Fabian &  
272 Leonhardt 2010; Monster et al. 2015b); the maximum allowed angle ( $\theta$ ) between the isolated  
273 NRM and acquired pTRM; and the intersection parameter ( $\Delta b$ ) (Monster et al., 2015b), which  
274 tests whether the linear fit regression line intersects the y-axis at the theoretically predicted  
275 value of  $-1$ . In order to confirm the obtained and only reliable results, we have set  $|\varepsilon_{\text{alt}}| \leq$   
276 5%,  $\theta$  must be less than  $10^\circ$ , and a threshold value of  $\Delta b$  is  $\pm 0.1$ . In the MSP-Tool software,  
277 the bootstrap statistics were applied to calculate the mean and 95% confidence intervals.

278 Technically, successful MSP experiments were obtained from profiles V and HT, while both  
279 HM and HB failed to give reliable estimates as their  $\varepsilon_{\text{alt}}$  parameter exceeded the defined  
280 limit. In V, three specimens out of nine were rejected (Fig. 5a) as they have altered during  
281 the MSP run. The remaining six met the criteria limit defined above and thus a domain state  
282 corrected PI mean of  $62.9 \pm 2.6 \mu\text{T}$  was obtained for the vertical profile. The HT gave

283 successful MSP experiment in eight out of ten specimens (Fig 5b), with PI value of  $58.6 \mu T$ ,  
284 after DSC procedure. We note here that 95% confidence interval in HT ( $+6.5/-6.3 \mu T$ ) is  
285 almost double the value of the confidence interval in V. Obviously, this high scatter is  
286 reasoned by the noticeable nonlinearity behavior, in the last field steps (Fig. 5b), between the  
287 TRM and applied magnetic field. This non-ideal behavior can be attributed to presence of  
288 large ferromagnetic particles, which can reduce the efficiency of linearity law (Selkin et al.,  
289 2007). Regarding to HM, only one specimen out of nine passed the alteration limit (Fig. 5c),  
290 indicating that most of the middle-zone specimens are susceptible to alteration. In addition,  
291 the last data points are not aligned linearly which probably point to the dominance of MD  
292 particles. Therefore, no reliable results were obtained from this profile.

293 We have neglected the criteria limits to obtain reliable results without regard to data quality,  
294 just to see the impact of the sample position in vertical profile on the PI results. A MSP-DSC  
295 value of  $67.2 \mu T$  was obtained, this is demonstrated in the supplementary Figure S1. Three  
296 accepted data out of nine (33% success rate) was found along HB profile (Fig. 5d) and thus  
297 no meaningful estimate could be obtained. As in HM, if we neglect the criteria set parameters  
298 (Fig. S2), a value of  $60.8 \mu T$  is calculated for HB profile.

299 From the above results, it is obvious that only the vertical and upper horizontal profiles gave  
300 reliable results that meet the proposed criteria limits. Therefore, combining all accepted  
301 specimens from V and HT enables us to assign Xite-mean PI (Fig. 6a) at  $60.5 (+4.0/-4.1)$   
302  $\mu T$ . Including all the 18 specimens of HM and HB (Fig. 6b) gives, unexpectedly, a mean  
303 value of  $63.8 (+5.2/-5.8) \mu T$ , which considering the uncertainty limits, is indistinguishable  
304 from the mean value calculated from only reliable results. This consistency may denote that  
305 the current conditions set for accepting the MSP results ( $\epsilon_{alt}$  and  $\Delta b$ ) are ineffective. Such

306 explanation, however, cannot be confirmed in this study, as the actual intensity value during  
307 Xitle eruption time (370 AD) is unknown. But, we can deduce that obtaining reliable MSP  
308 results for a certain lava unit could be achieved by taking many specimens as possible from  
309 different parts within the lava flow. However, these approaches will cost effort and time.

## 310 **6. Discussion**

311 Three horizontal profiles were sampled from Xitle in three levels from bottom to top in order  
312 to discuss horizontal variations of paleointensity. Horizontal characteristics along these  
313 profiles were investigated as well through sampling one vertical profile of *ca.* 4.5 m  
314 thickness. Rock magnetic experiments were completed to infer the type and size of the  
315 ferromagnetic minerals and their thermal stability. It must be mentioned that the number of  
316 present samples that have undergone magnetic experiments and MSP run are few and uneven,  
317 and thus the relationship between magnetic properties and paleointensity behavior along  
318 lava's profile may not be clear. However is not the main focus of this study, as we here try  
319 to enhance the PI estimates of Xitle by evaluating previous data and conducting a new MSP  
320 experiment. Completing this, we can provide an average value with low confidence limit,  
321 through combining present PI results with reliable results obtained from previous studies.  
322 Despite the limited number of data, we can give a general overview of the impact of lava  
323 position and its physical and magnetic properties on the MSP results. Currently, few studies  
324 have addressed the relation between rock magnetic properties and lava flow thickness. Some  
325 studies (Coe et al., NATURE, 1995; Rolph, 1997; Hill and Shaw, 2000; V  rard et al., 2012)  
326 have discussed this relation on thin lava flows, thickness < 2 m, some others extended these  
327 studies to thicker lavas of ~6m long (B  hnel et al., 1997; de Groot et al., 2014), and up to  
328 several tens of meters (e.g. Wilson et al., 1968; Audunssen et al., 1992). Findings from these

329 studies indicate an effect of the sampling location on the magnetic properties. Lava thickness  
330 reflects different cooling history, the top and bottom parts cooled faster than the central part  
331 of the flow. These variations in cooling time govern the size of the ferromagnetic crystals  
332 and their oxidations states. The top part of the lava flows may produce smaller ferromagnetic  
333 sensus lato particles with lower oxidation state in comparison to those formed in the middle  
334 of the flow (see for example Böhnel et al., 1997; de Groot et al., 2014).

335 Böhnel et al. (1997) showed detailed results of Xitle's rock magnetic properties (i.e. Tc,  
336 magnetic susceptibility, hysteresis parameters, and coercivities) and PIs along a vertical  
337 profile of 6 m thickness. Results indicate that, unlike magnetic properties, the PIs seem to  
338 have a systematic behavior with tendency of middle flow samples to give larger PI variations  
339 in comparison to the top and bottom samples. Despite the detailed study, they did not find  
340 meaningful relation between PI variations and physical and magnetic properties. Our  
341 sampled profile spaced only (0.96 km) from Böhnel et al. (1997) profile, implying that they  
342 shared almost the same cooling history. The rock-magnetic experiments done in this study  
343 showed that Ti-poor T<sub>Mt</sub> and/or M<sub>t</sub> is the dominant ferromagnetic mineral(s) and few  
344 hematite is present, showed from *k*-T curves (Fig. 4a). These minerals are located broadly on  
345 the PSD size with wide range of MDF ( from *ca.* 5 to 56 mT). From top to bottom (V), and  
346 along each horizontal profile (HT, HM, HB), we do not find any systematic changes on the  
347 magnetic properties although of the, above mentioned, differences in cooling times. Although  
348 the magnetic parameters obtained in this study varied (e.g. RP%, MDF and MDT)  
349 horizontally, we consider that they do not reflect true magnetic properties changes, as the  
350 cooling time and content of the cooled lava on such a small scale (1.5 m) are seemingly  
351 constant, at least in comparison to vertical direction. This discrepancy in magnetic data could



352 be attributed to the limited number of rock magnetic experiments carried out. In conclusion,  
353 there is not a direct connection found between lava thickness and its 1.5 m lateral extent with  
354 the magnetic properties.

355 Now, we discuss the influence of cooling time on the MSP results. Our contributed results  
356 show that the topmost horizontal profile and the vertical profile have yielded successful MSP-  
357 DSC PI determinations from the 14 selected samples out of 19 available (74% success rate).  
358 On the hand, samples from central and bottom parts of the flow do not give satisfactory MSP  
359 results, as they have exceeded the limits of criteria set designed following Monster et al.  
360 (2015). Apparently, getting differential MSP results and success rate from over a flow section  
361 of 4.5 m thickness can be directly related to the cooling time of this flow. It means that top  
362 part of the Xitle flow is appropriate for conducting MSP experiments as it has cooled faster  
363 than underlying horizontal sections. Moreover, conducting the experiment vertically does  
364 give almost the same results given from HT profile (Fig. 5a and b), which could indicate that  
365 the effect of cooling time on MSP results may be insignificant or even disappeared if samples  
366 are taken vertically. This explanation is based on a few number of samples and more studies  
367 are needed to emphasize it. From these notes, we recommend sampling a lava flow  
368 horizontally from its top part when the lava flow is not covered by a younger flow, and  
369 vertically in order to give a reliable MSP estimates.

370

371

## 372 **7. Conclusions**

373 The rock magnetic properties indicate that the main magnetic minerals are Ti-poor  
374 titanomagnetite with small contribution from hematite of PSD carriers accomplish the quality

375 criterion to be able for paleointensity experiments.  
376 Successful MSP-DSC experiments were obtained from profiles V and HT, while both HM  
377 and HB failed to give reliable estimates. Results obtained in this study from 14 accepted  
378 specimens of HT and V profiles give an average mean for Xitle at  $60.5 (+4.0/-4.1) \mu T$ . This  
379 value constrains greatly the dispersion and we consider it should substitute the value for the  
380 Xitle from the database used by models in order to do more precise the secular variation  
381 curve used for the dating of geologic and archeomagnetic materials of this period.  
382 This mean value is consistent with the mean ( $62.0 \pm 9.3 \mu T$ ) calculated from 134 filtered  
383 Thellier & microwave old PI data. The whole PI mean value for Xitle, using a combined  
384 formula (Higgins and Green, 2011) gives  $61.9 \pm 9 \mu T$ . This mean value is calculated from  
385 high quality data provided from three different PI methods, therefore most likely represents  
386 the intensity value for Central Mexico at *ca.* 370 AD.

387

388

### 389 **Acknowledgments**

390 We appreciate the financial support to L. M. Alva-Valdivia from PAPIIT-DGAPA-UNAM  
391 IN113117 and ANR-CONACyT (France-Mexico) 273564, research projects. AN Mahgoub  
392 acknowledged the financial support of the Universidad Nacional Autónoma de México-  
393 postdoctoral fellowship. M. A. Bravo-Ayala was partly financially supported by a  
394 scholarship from CONACyT and a Research Grant from Dr. P. Camps and Dr. T. Poidrás  
395 whom allowed the use of the Paleomagnetic laboratory of Geoscience University of  
396 Montpellier, France. Thanks to J. A. González Rangel for the support on the Mexican  
397 Paleomagnetic laboratory experiments.

398

399

400

401

402

403 **References**

- 404 Aitken, M., Allsop, A., Bussell, G., Winter, M., 1988. Determination of the intensity of the  
405 Earth's magnetic field during archaeological times: Reliability of the Thellier  
406 technique. *Rev. Geophys.* 26 (1), 3–12.
- 407 Alva-Valdivia, L., 2005, Comprehensive paleomagnetic study of a succession of Holocene  
408 olivine-basalt flow: Xitle Volcano (Mexico) revisited, *Earth Planets Space*, Vol. 57,  
409 pp. 869-853.
- 410 Audunssen, H., S. Levi, and F. Hodges (1992), Magnetic property zonation in a thick lava  
411 flow, *J. Geophys. Res.*, 97(B4), 4349–4360.
- 412 Biggin, A.J., Steinberger, B., Aubert, J., Suttie, N., Holme, R., Torsvik, T.H., van der Meer,  
413 D.G., van Hinsbergen, D.J.J. (2012) Possible links between long-term geomagnetic  
414 644 variations and whole-mantle convection processes. *Nat Geosci* 5:526–533
- 415 Biggin, A.J., Böhnell, H.N. & Zuniga, F.R., 2003. How many paleointensity determinations  
416 are required from a single lava flow to constitute a reliable average? *Geophys. Res.*  
417 *Lett.*, 30(11).
- 418 Böhnell, H., Morales, J., Caballero, C., Alva, L., McIntosh, G., González, S. y Sherwood, J.,  
419 1997, Variation of rock magnetic parameters and paleointensities over a single  
420 holocene lava flow, *J. Geomag. Geoelectr.*, 49, 523 - 542.
- 421 Böhnell, H., E. Herrero-Bervera, and M. J. Dekkers (2011), Paleointensities of the Hawaii  
422 1955 and 1960 Lava Flows: Further Validation of the Multi-specimen Method, pp.  
423 195–211, Springer, Dordrecht, Netherlands.
- 424 Böhnell, H., A. J. Biggin, D. Walton, J. Shaw, and J. A. Share (2003), Microwave  
425 palaeointensities from a recent Mexican lava flow, baked sediments and reheated  
426 pottery, *Earth Planet. Sci. Lett.*, 214, 221–236.
- 427 Coe, R.S., 1967. Paleo-intensities of the Earth's magnetic field determined from Tertiary  
428 and Quaternary rocks. *J. Geophys. Res.* 72 (12), 3247–3262.
- 429 Coe RS, Grommé S, Mankinen EA (1978) Geomagnetic paleointensities from radiocarbon  
430 dated lava flows on Hawaii and the question of the Pacific nondipole low. *J Geophys*  
431 *Res Solid Earth* 83(B4):1740–1756

432 Cromwell, G., Tauxe, L., Staudigel, H., Ron, H., 2015. PI estimates from historic and  
433 modern Hawaiian lava flows using glassy basalt as a primary source material.  
434 *Phys. Earth Planet. Inter.* 241, 44–56.

435 de Groot, L. V., T. A. T. Mullender, and M. J. Dekkers (2013), An evaluation of the influence  
436 of the experimental cooling rate along with other thermomagnetic effects to explain  
437 anomalously low palaeointensities obtained for historic lavas of Mt Etna (Italy),  
438 *Geophys. J. Int.*, 193(3), 1198–1215, doi:10.1093/gji/ggt065.

439 de Groot, L.V., Dekkers, M.J., Visscher, M., ter Maat, G.W., 2014. Magnetic properties and  
440 paleointensities as function of depth in a Hawaiian lava flow. *Geochem. Geophys.*  
441 *Geosyst.* 15. <http://dx.doi.org/10.1002/2013GC005094>.

442 Day, R., Fuller, M., Schmidt, V.A., 1977. Hysteresis properties of titanomagnetites: grain  
443 size and compositional dependence. *Phys. Earth Planet. Inter.* 13, 260–267.

444 Dekkers, M.J., Böhnell, H.N., 2006. Reliable absolute palaeointensities independent of  
445 magnetic domain state. *Earth Planet. Sci. Lett.* 284, 508-517.

446 Dunlop, D.J., 2002. Theory and application of the Day plot (Mrs/Ms versus Hcr/Hc) 1.  
447 Theoretical curves and tests using titanomagnetite data. *J. Geophys. Res.* 107(B3)  
448 2056. doi:10.1029/2001JB000486.

449 Fabian, K., Leonhardt, R., 2010. Multiple-specimen absolute PI determination: An optimal  
450 protocol including pTRM normalization, domain-state correction, and alteration test.  
451 *Earth Planet. Sci. Lett.* 297, 84–94.

452 Gonzalez S, Sherwood GJ, Boehnel H, Schnepf E (1997), Paleosecular variation in central  
453 Mexico over the last 30,000 years: The record from lavas. *Geophys J Int* 130:  
454 201– 219.

455 González, S., Pastrana, A., Siebe, C., Duller, G., 2000. Timing of the prehistoric eruption of  
456 Xitle volcano and the abandonment of Cuicuilco pyramid, southern Basin of Mexico.  
457 *Geol. Soc. London Sp. Pub.* 171, 205-224.  
458 <https://doi.org/10.1144/GSL.SP.2000.171.01.17>.

459 Grappone, J.M., Biggin, A.J., Hill. M.J., 2019: Solving the mystery of the 1960 Hawaiian  
460 lava flow: implications for estimating Earth’s magnetic field. *Geophys. J. Int.*, 218,  
461 1796–1806.

462 Guilbaud, M.N., Siebe, C., Layer, P., Salinas, S., 2012. Reconstruction of the volcanic history  
463 of the Tacámbaro-Puruarán area (Michoacán, México) reveals high frequency of  
464 Holocene monogenetic eruptions. *Bull. Volcanol.* 74, 1187–1211.

465

466 Heizer, R.F., Bennyhoff, J.A., 1958. Archeological investigations of Cuicuilco, Valley of  
467 Mexico, 1957. *Science* 127, 232±233.

468 Higgins J and Green S. *Cochrane Handbook for Systematic Reviews of Interventions*  
469 Version 5.1.0. The Cochrane Collaboration, 2011, [www.handbook.cochrane.org](http://www.handbook.cochrane.org).

470 Hill, M. J., and J. Shaw (1999), Palaeointensity results for historic lavas from Mt Etna using  
471 microwave demagnetization/remagnetization in a modified Thellier-type  
472 experiment, *Geophys. J. Int.*, 139(2), 583–590

473 Hill, M. J., and J. Shaw (2000), Magnetic field intensity study of the 1960 Kilauea lava flow,  
474 Hawaii, using the microwave PI technique, *Geophys. J. Int.*, 142, 487–504.

475 Luhr, J.F., Simkin, T., 1993. *Paricutin: The Volcano Born in a Mexican Cornfield*.  
476 Geoscience Press (427 p).

477 Mahgoub, A.N., Juárez-Arriaga, E., Böhnel, H., Manzanilla, L.R., Cyphers, A., 2019.  
478 Refined 3600 years palaeointensity curve for Mexico. *Phys. Earth Planet. Inter.*  
479 Accepted.

480 Morales, J., Alva-Valdivia, L., Goguitchaichvili, A. y Urrutia-Fucugauchi, J., 2006, Cooling  
481 rate corrected paleointensities from the Xitle lava flow: Evaluation of within-site  
482 scatter for single spot-reading cooling units, *Earth Planets Space*, Vol. 58, pp. 1341-  
483 1347.

484 Morales, J., Goguitchaichvili, A. y Urrutia-Fucugauchi, J., 2001, A rock-magnetic and PI  
485 study of some Mexican volcanic lava flows during the Latest Pleistocene to the  
486 Holocene, *Earth Planets Space*, Vol. 53, pp. 893–902.

487 Monster, M.W.L., de Groot, L.V., Biggin, A.J., Dekkers, M.J., 2015a. The performance of  
488 various PI techniques as a function of rock magnetic behaviour – a case study for  
489 La Palma. *Phys. Earth Planet. Inter.* 242, 36–49. [http://dx.doi.org/10.1016/](http://dx.doi.org/10.1016/j.pepi.2015.03.004)  
490 [j.pepi.2015.03.004](http://dx.doi.org/10.1016/j.pepi.2015.03.004)

491 Monster, M.W.L., de Groot, L.V., Dekkers, M.J., 2015b. MSP-tool: a VBA-based software  
492 tool for the analysis of multispecimen PI data. *Front. Earth Sci.* 3, 86.  
493 <http://dx.doi.org/10.3389/feart.2015.00086>.

494 Nagata, T., Kobayashi, K., Schwarz, E.J., 1965. Archaeomagnetic intensity studies of South  
495 and Central America. *J. Geomagnetism Geoelectricity*, 17, 399-405,  
496 <https://doi.org/10.5636/jgg.17.399>

497

498 Nilsson A, Holme R, Korte M, Suttie N, Hill M (2014) Reconstructing Holocene  
499 geomagnetic field variation: New methods, models and implications. *Geophys J Int*  
500 198(1):229–248

501 Paterson GA, Tauxe L, Biggin AJ, Shaar R, Jonestrask LC (2014) On improving the 843  
502 selection of Thellier-type paleointensity data. *Geochem Geophys Geosyst* 15(4):  
503 1180–844 1192

504 Paterson, G. A., L. Tauxe, A. J. Biggin, R. Shaar, and L. C. Jonestrask (2014), On improving  
505 the selection of Thellier-type paleointensity data, *Geochem. Geophys. Geosyst.*, 15,  
506 1180–1192, doi:10.1002/2013GC005135.

507 Pavón-Carrasco, F.J., Osete, M.L., Torta, J.M., De Santis, A., 2014. A geomagnetic field  
508 model for the Holocene based on archaeomagnetic and lava flow data. *Earth Planet.*  
509 *Sci. Lett.* 388, 98–109.

510 Pioli, L., Erlund, E., Johnson, E., Cashman, K.V., Wallace, P., Rosi, M., Delgado, H., 2008.  
511 Explosive dynamics of violent Strombolian eruptions: the eruption of Parícutin  
512 volcano 1943–1952 (Mexico). *Earth Planet. Sci. Lett.* 271 (1–4), 359–368.

513 Rasoazanamparany, C., Widom, E., Siebe, C., Guilbaud, M.-N., Spicuzza, M.J., Valley, J.W.,  
514 Valdez, G., Salinas, S., 2016. Temporal and compositional evolution of Jorullo  
515 volcano, Mexico: implications for magmatic processes associated with a  
516 monogenetic eruption. *Chem. Geol.* 434, 62–80.

517 Rolph, T.C., 1997. An investigation of the magnetic variation within two recent lava flows,  
518 *Geophys. J. Int.*, 130, 125–136.

519 Roberts, A.P., Tauxe, L., Heslop, D., Zhao, X., Jiang, Z., 2018. A critical appraisal of the  
520 Day diagram. *J. Geophys. Res.* 123, 2618–2644.  
521 <https://doi.org/10.1002/2017JB015247>.

522 Selkin, P. A., J. S. Gee, and L. Tauxe (2007), Nonlinear thermoremanence acquisition and  
523 implications for PI data, *Earth Planet. Sci. Lett.*, 256, 81–89,  
524 doi:10.1016/j.epsl.2007.01.017.

525 Siebe, C., 2000. Age and archaeological implications of Xitle volcano, southwestern Basin  
526 of Mexico-City. *J. Volcanol. Geotherm. Res.* 104, 45-64.  
527 [https://doi.org/10.1016/S0377-0273\(00\)00199-2](https://doi.org/10.1016/S0377-0273(00)00199-2).

528 Shaw, J., 1974, A new method of determining the magnitude of the paleomagnetic field  
529 application to 5 historic lavas and five archeological samples. *Geophysical Journal*  
530 *of the Royal Astronomical Society* 39: 133-141. doi: 10.1111/j.1365-  
531 246X.1974.tb05443.x.

532 Stacey, F.D. & Banerjee, S.K., 1974. *The Physical Principles of Rock Magnetism*, Elsevier,  
533 Amsterdam.

534

535 Tauxe, L., T. Pick, and Y. Kok (1995), Relative PI in sediments: A pseudo-Thellier approach,  
536 *Geophys. Res. Lett.*, 22(21), 2885–2888.

537 Thellier, E. & Thellier, O., 1959. Sur l'intensité du champ magnétique terrestre dans le  
538 passé historique et géologique, *Ann Géophys.*, 15, 285–376.

539 Tauxe, L., Staudigel, H., 2004. Strength of the geomagnetic field in the Cretaceous Normal  
540 Superchron: new data from submarine basaltic glass of the Troodos Ophiolite.  
541 *Geochem. Geophys. Geosyst.* 5 (Q02H06).

542 Tsunakawa, H., Shaw, J., 1994. The Shaw method of PI determinations and its application to  
543 recent volcanic rocks. *Geophys. J. Int.* 118, 781–787.

544 Urrutia Fucugauchi, J., 1996. Palaeomagnetic study of the Xitle- Pedregal de San Angel lava  
545 flow, southern Basin of Mexico. *Physics of the Earth and Planetary Interiors* 97, 177-  
546 196.

547 Verard, C., R. Leonhardt, and M. Winklhofer (2012), Variations of magnetic properties in  
548 thin lava flow profiles: Implications for the recording of the Laschamp Excursion,  
549 *Phys. Earth Planet. Inter.*, 200–201, 10–27, doi:10.1016/j.pepi.2012.03.012.

550 Walton, D., Share, J.A., Rolph, T.C. & Shaw, J., 1993. Microwave magnetisation, *Geophys.*  
551 *Res. Lett.*, 20, 109–111.

552 Wilson, R. L., S. E. Haggerty, and N. D. Watkins (1968), Variation of palaeomagnetic  
553 stability and other parameters in a vertical traverse of a single Icelandic lava,  
554 Geophys. J. R. Astron. Soc., 16, 79–96.

555 Yamamoto, Y., Tsunakawa, H. & Shibuya, H., 2003. Palaeointensity study of the Hawaiian  
556 1960 lava: implications for possible causes of erroneously high intensities, Geophys.  
557 J. Int., 153(1), 263–276.

558

559

560

561 List of Figures

562

563 **Figure 1.** Distribution of Xitle lava flows I to VI, with the location of the sampling site and  
564 the Cuicuilco archeological site. Modified after Delgado et al. (1998).

565 **Figure 2.** Evaluation of previous PI data published for Xitle. The closed and open circles  
566 represent reliable and unreliable data based on a set of selection criteria designed in this study  
567 (see section 2). The dotted line and shaded area is the Xitle mean paleointensity value and  
568 95% standard deviation, calculated from only reliable data. the x-axis represent different  
569 studies that were done on Xitle.

570 for abbreviations: *Nag-65* is Nagata et al. (1965); *UFT-96* is Urrutia-Fucugauchi (1996),  
571 from thellier experiment; *UFS-96* is Urrutia-Fucugauchi (1996) from Shaw experiment; *BH-*  
572 *97* is Böhnell et al. (1997); *GZT-97* is Gonzales et al. (1997) from thellier; *GZS-97* is Gonzales  
573 et al. (1997) from Shaw; *M-01* is Morales et al. (2001); *BHT-03* is Böhnell et al. (2003) from  
574 thellier after re-analyzing data of Böhnell et al. (1997); *BHMI-03* is Böhnell et al. (2003) from  
575 microwave done on lavas; *BHMP-03* is Böhnell et al. (2003) from microwave done on  
576 potteries; *LA-05* is Alva-Valdivia (2005); *M-06* is Morales et al. (2006); and *MG-19* is  
577 Mahgoub et al. (2019, accepted for publication).

578

579 **Figure 3.** Sampling profile. Lava flow with scale (1m). Three zones are observed with the  
580 naked eye: the massive central zone and the upper zone that present abundant vesicles and  
581 lower with much less and tiny vesicles. The core numbers are shown in order to be compared  
582 with upcoming rock magnetic properties and paleointensities.



583

584 **Figure 4.** Rock magnetic results done in this study: (a) susceptibility vs. temperature curves;  
585 (b) Day plot (Day et al., 1977) with thresholds for single domain (SD), pseudo single domain  
586 (PSD), and multidomain (MD) shown as straight grey lines. Dashed curved lines represent  
587 the SD-MD theoretical mixing curves, after Dunlop (2002); (c) intensity decay curves  
588 obtained after alternating field demagnetization; (d) intensity decay curves after thermal  
589 demagnetization. Numbers in each panel diagram represent core sample, see Figure 3.  
590 AHMED, LAS CURVAS EN 4A CASI NO SE VEN. Y EN 4C Y 4D EL EJE Y DEBE SER  
591 NORMALIZED MAGNETIZATION.

592

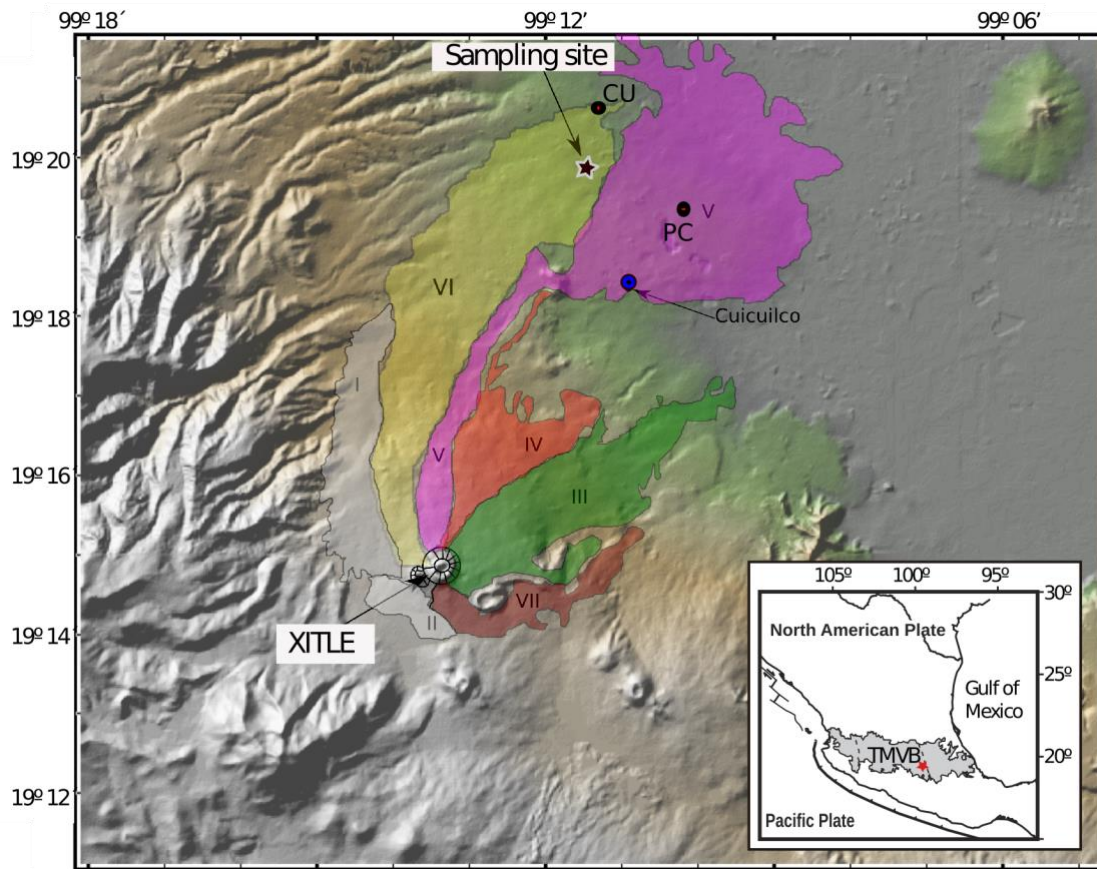
593 **Figure 5.** Multispecimen results obtained from four sampled profiles, after domain state  
594 correction (DSC). In each DSC protocol, the average alteration parameter ( $\epsilon_{alt}$ ) and the  
595 intersection criterion ( $\Delta b$ ) are demonstrated to judge the credibility of the given results. Note  
596 that data were analyzed with MSP-Tool software (Monster et al., 2015b) where bootstrap  
597 statistics were applied to calculate the mean (solid black line) and 95% confidence interval  
598 (dashed black lines lines). Black and orange circles represent those accepted and unaccepted  
599 data, respectively, based on the criteria limit defined in the present study. (a and b) represent  
600 accepted experiments done on profiles V and HT, as their specimens meet the designed  
601 criteria limit, and (c and d) represent unaccepted experiments from profiles HM and HB and  
602 thus no PI mean could be calculated from these two profiles.

603

604 **Figure 6.** (a) Xitle PI mean value calculated from only reliable experiments done on V and  
605 HT profiles. (b) represents unreliable experiments (from profiles HM and HB), and the  
606 bootstrap mean (solid black line) and 95% confidence interval (dashed black lines lines) are  
607 shown to compare the Pi results obtained from reliable (a) and unreliable (b) data.

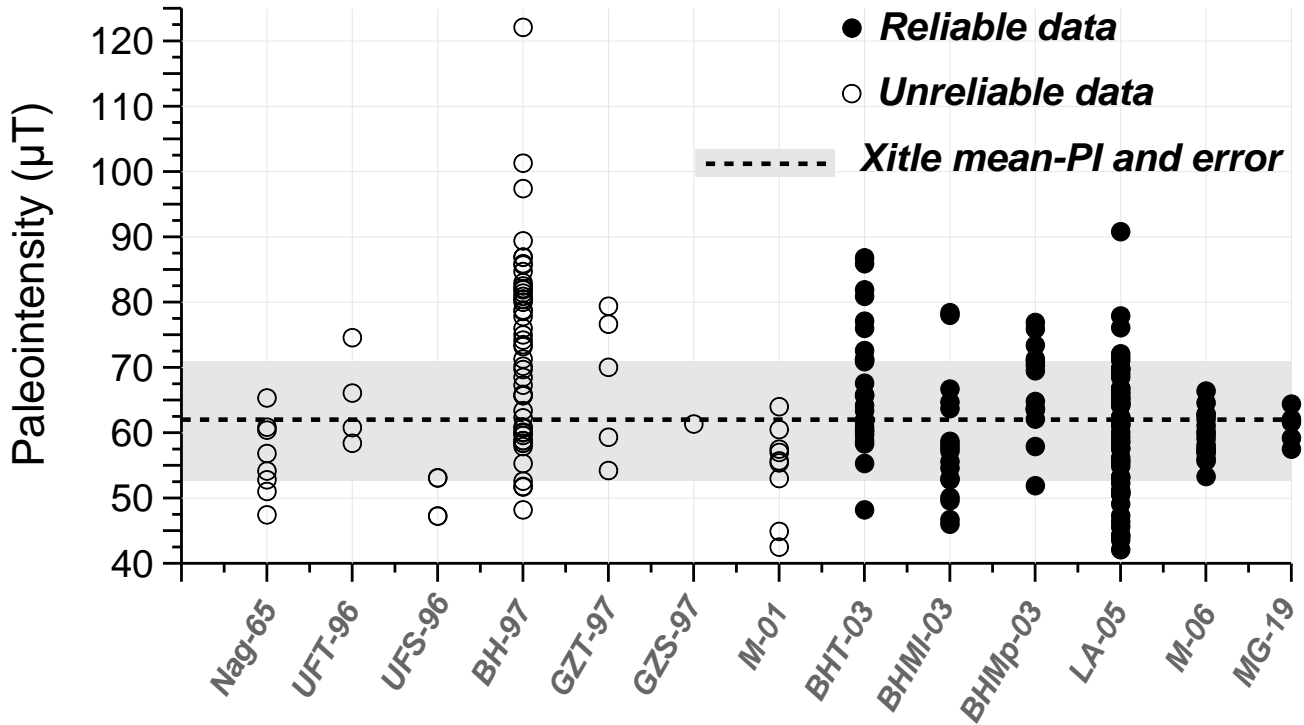
608

609



610  
 611  
 612  
 613  
 614  
 615  
 616  
 617  
 618  
 619

**Figure 1.** Distribution of Xitle lava flows I to VI, with location of the sampling site and Cuicuilco archeological site. Modified after Delgado et al. (1998). WE ARE STILL WORKING ON THIS FIGURE!



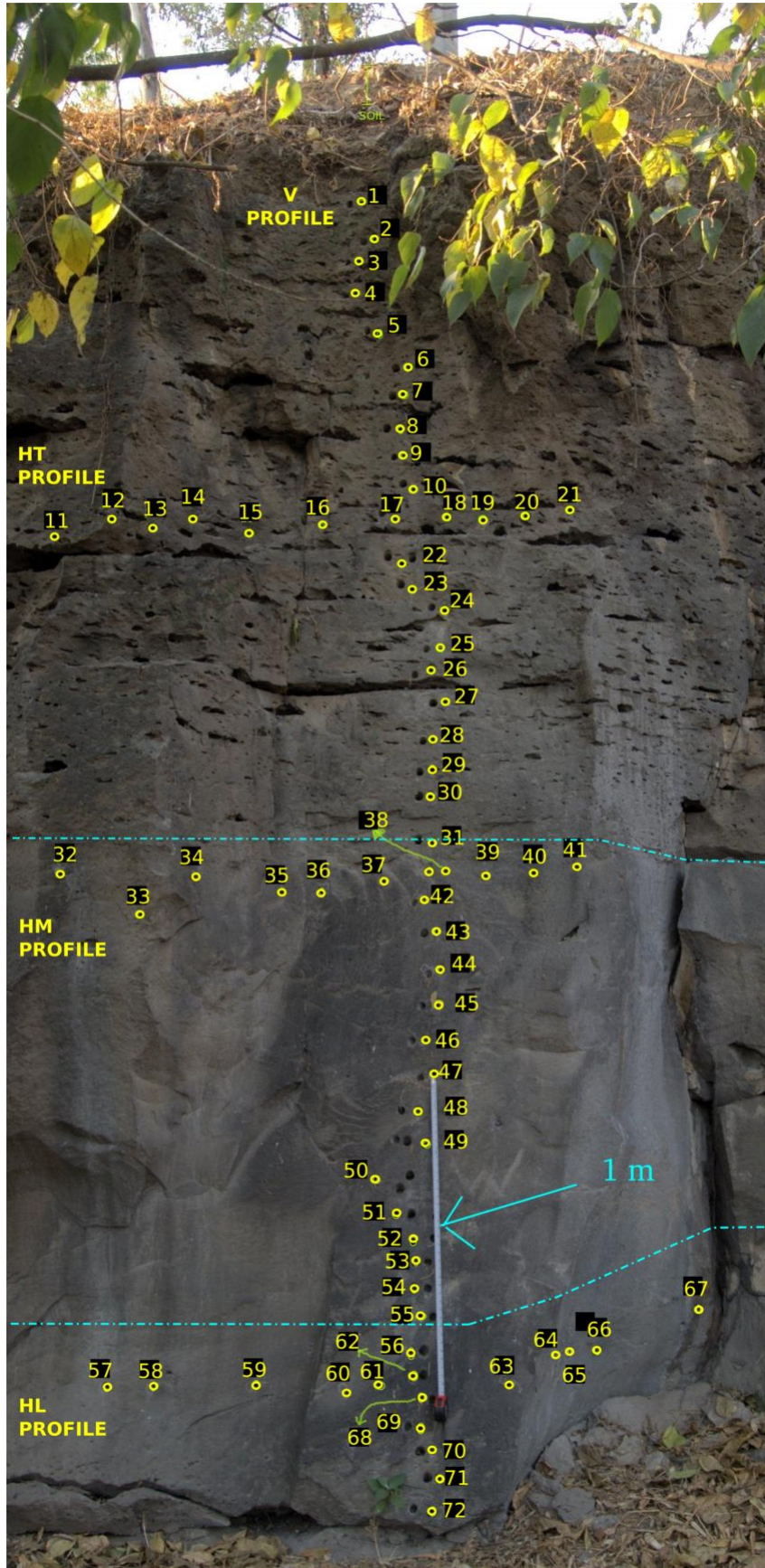
620

621

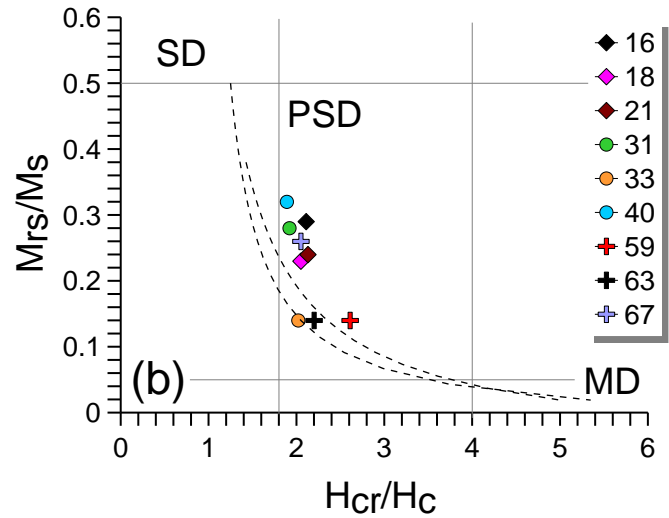
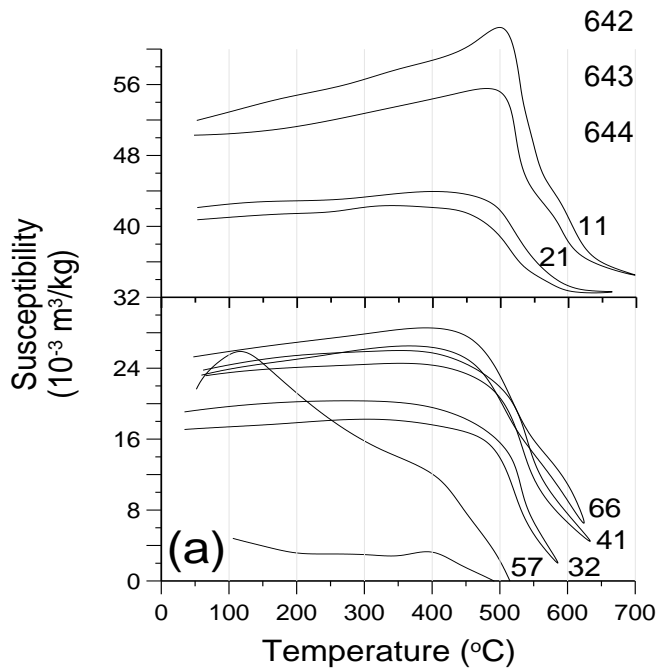
622

623 Figure 2. Evaluation of previous PI data published for Xitle. The closed and open circles  
 624 represent reliable and unreliable data based on a set of selection criteria designed in this study  
 625 (see section 2). The dotted line and shaded area is the Xitle mean paleointensity value and  
 626 95% standard deviation, calculated from only reliable data. the x-axis represent different  
 627 studies that were done on Xitle.

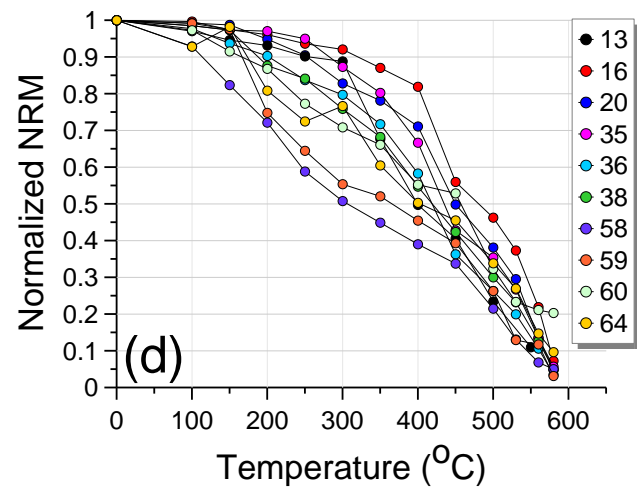
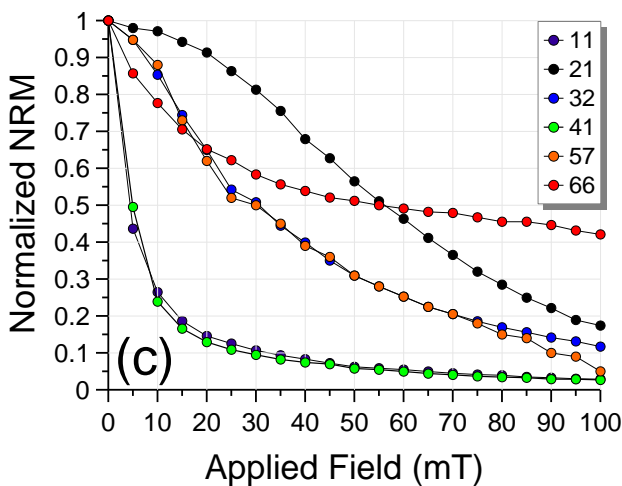
628 for abbreviations: *Nag-65* is Nagata et al. (1965); *UFT-96* is Urrutia-Fucugauchi (1996),  
 629 from thellier experiment; *UFS-96* is Urrutia-Fucugauchi (1996) from Shaw experiment; *BH-*  
 630 *97* is Böhnel et al. (1997); *GZT-97* is Gonzales et al. (1997) from thellier; *GZS-97* is Gonzales  
 631 et al. (1997) from Shaw; *M-01* is Morales et al. (2001); *BHT-03* is Böhnel et al. (2003) from  
 632 thellier after re-analyzing data of Böhnel et al. (1997); *BHMI-03* is Böhnel et al. (2003) from  
 633 microwave done on lavas; *BHMP-03* is Böhnel et al. (2003) from microwave done on  
 634 potteries; *LA-05* is Alva-Valdivia (2005); *M-06* is Morales et al. (2006); and *MG-19* is  
 635 Mahgoub et al. (2019, accepted for publication).



637 **Figure 3.** Sampling profile. Lava flow with scale (1m). Three zones are observed with the  
638 naked eye: the massive central zone and the upper and lower zones that present vesicles. The  
639 core numbers are shown in order to be compared with upcoming rock magnetic properties  
640 and paleointensities.  
641



645

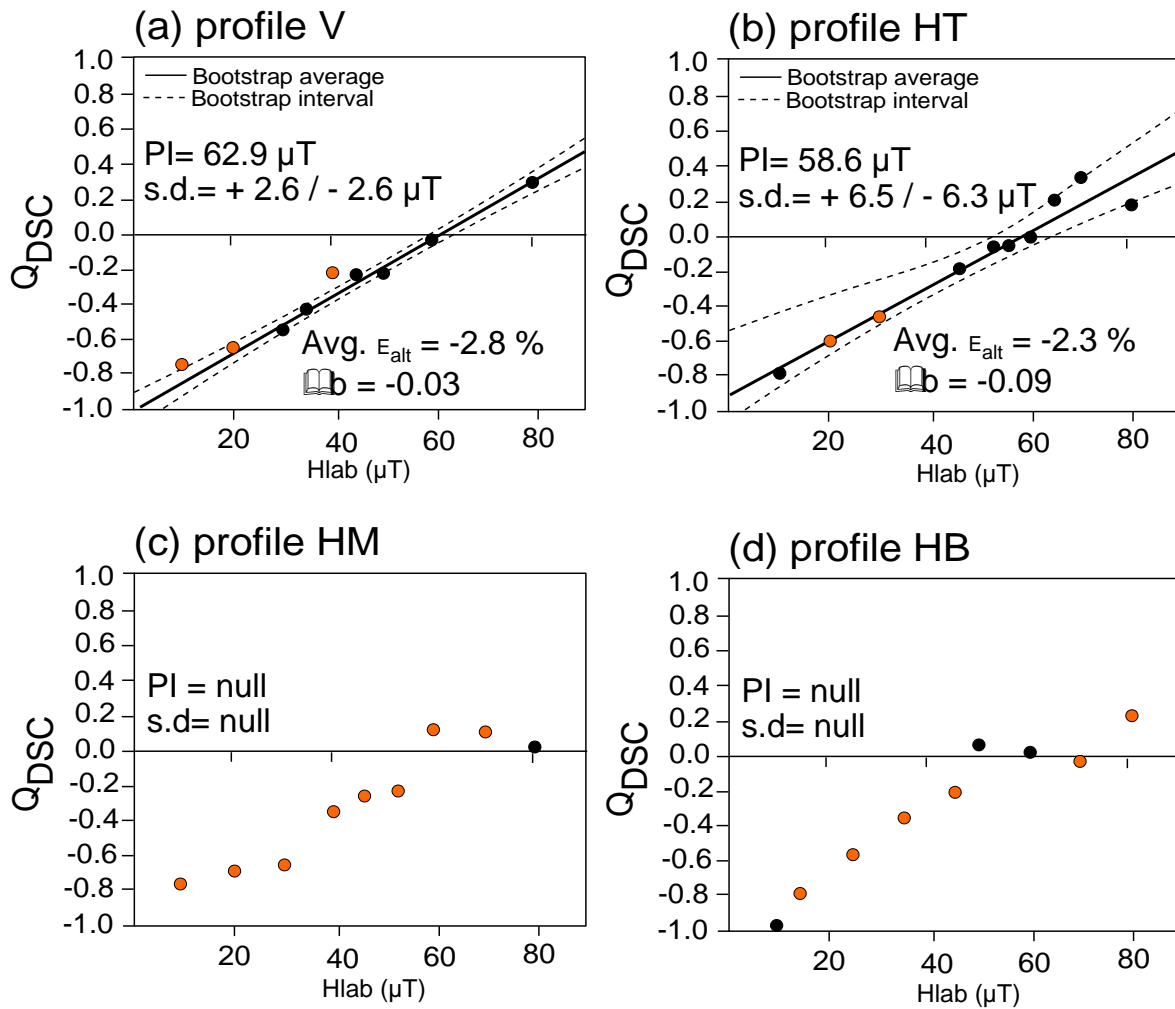


646

647

648 **Figure 4.** Rock magnetic results done in this study: (a) susceptibility vs. temperature curves;  
 649 (b) Day plot (Day et al., 1977) with thresholds for single domain (SD), pseudo single domain  
 650 (PSD), and multidomain (MD) shown as straight grey lines. Dashed curved lines represent  
 651 the SD-MD theoretical mixing curves, after Dunlop (2002); (c) intensity decay curves  
 652 obtained after alternating field demagnetization; (d) intensity decay curves after thermal  
 653 demagnetization. Numbers in each panel diagram represent core sample, see Figure 3.

654



655

656

657

658

659

660 **Figure 5.** Multispecimen results obtained from four sampled profiles, after domain state  
 661 correction (DSC). In each DSC protocol, the average alteration parameter ( $\epsilon_{\text{alt}}$ ) and the  
 662 intersection criterion ( $\Delta b$ ) are demonstrated to judge the credibility of the given results. Note  
 663 that data were analyzed with MSP-Tool software (Monster et al., 2015b) where bootstrap  
 664 statistics were applied to calculate the mean (solid black line) and 95% confidence interval  
 665 (dashed black lines). Black and orange circles represent those accepted and unaccepted  
 666 data, respectively, based on the criteria limit defined in the present study. (a and b) represent  
 667 accepted experiments done on profiles V and HT, as their specimens meet the designed

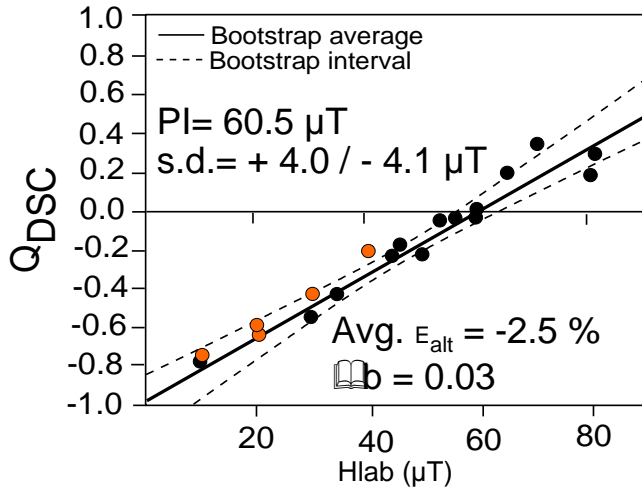
668 criteria limit, and (c and d) represent unaccepted experiments from profiles HM and HB and  
669 thus no PI mean could be calculated from these two profiles.

670

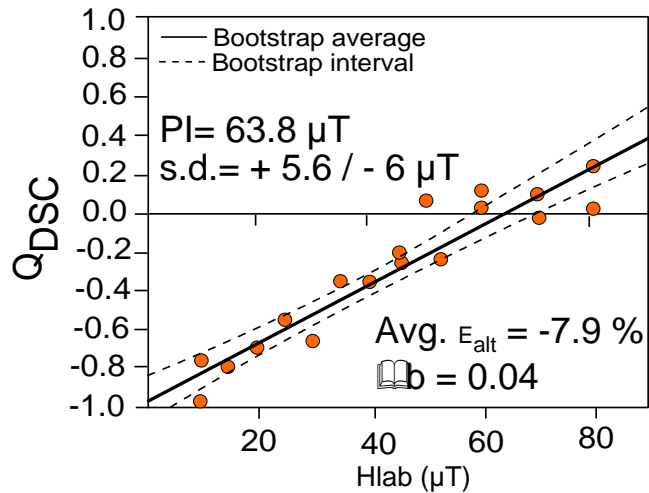


671

(a) Reliable experiment:  
V+HT



(b) Unreliable experiment:  
HB+HM



672

673

674

675

676 **Figure 6.** (a) Xitle PI mean value calculated from only reliable experiments done on V and

677 HT profiles. (b) represents unreliable experiments (from profiles HM and HB), and the

678 bootstrap mean (solid black line) and 95% confidence interval (dashed black lines) are

679 shown to compare the Pi results obtained from reliable (a) and unreliable (b) data

680

681

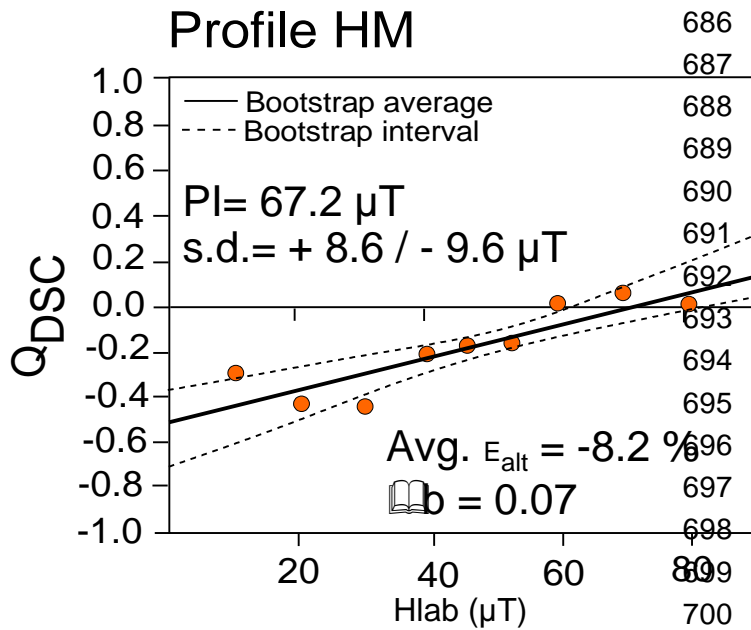
682

## Supplementary Materials

683

684 The supplementary materials consist of two figures.

685



701

702 Figure S1. Multispecimen results obtained from central profile (HM), after domain state  
703 correction (DSC). The data were analyzed with MSP-Tool software (Monster et al., 2015b)  
704 where bootstrap statistics were applied to calculate the mean (solid black line) and 95%  
705 confidence interval (dashed black lines lines). We note that in this profile we do not apply  
706 the selection criteria defined in the present study, as we just need to compare the unreliable  
707 data with reliable data.

708

709

710

711

712

713

714

715

716

717

718

719

720

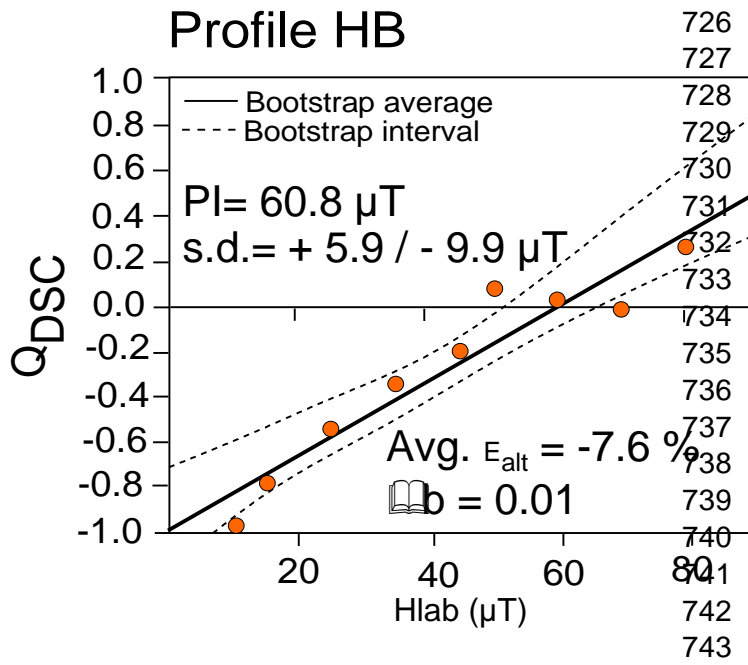
721

722

723

724

725



744 Figure S2. Multispecimen results obtained from bottom profile (HB). For details see Fig.  
745 S2 caption.

746

747